All-Carbon Electrode Molecular Electronic Devices based on Langmuir-Blodgett Monolayers

Soraya Sangiao[†‖], Santiago Martín[‡§], Alejandro González-Orive[†], César Magén[†‖‼], Paul J. Low[⊥], José M. de Teresa[†‡‖*], Pilar Cea[†§*]

[†] Instituto de Nanociencia de Aragón (INA), Fundación INA, and Laboratorio de Microscopias Avanzadas (LMA), Edificio I+D. Campus Rio Ebro, Universidad de Zaragoza, C/ Mariano Esquillor, s/n, 50018 Zaragoza, Spain.

[‡] Instituto de Ciencia de Materiales de Aragón (ICMA), Universidad de Zaragoza-CSIC, Campus Plaza San Francisco, 50009 Zaragoza, Spain.

[§] Departamento de Química Física, Facultad de Ciencias, Campus Plaza San Francisco, Universidad de Zaragoza, 50009, Zaragoza, Spain.

[‖] Departamento de Física de la Materia Condensada, Facultad de Ciencias, Campus Plaza San Francisco, Universidad de Zaragoza, 50009, Zaragoza, Spain.

[‼] Fundación ARAID, 50018 Zaragoza, Spain.

[⊥] School of Chemistry and Biochemistry, University of Western Australia, Crawley, 6009, WA, Australia.

Graphical Abstract

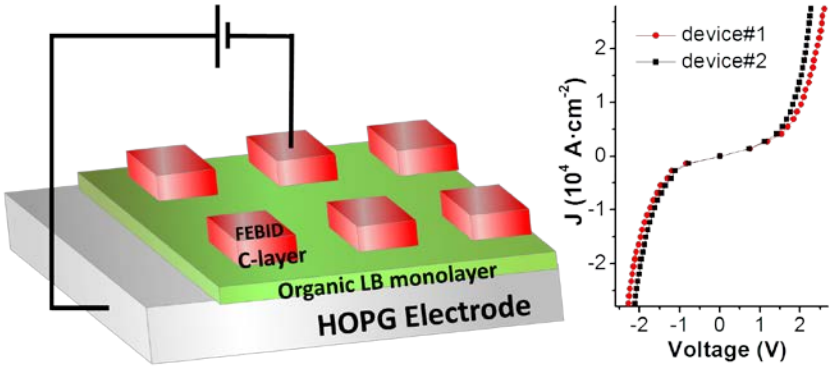

All-carbon electrode molecular electronic devices comprising a Langmuir-Blodgett monolayer of an organic 'molecular wire' sandwiched between two carbonaceous electrodes have been fabricated. The bottom electrode was highly oriented pyrolytic graphite (HOPG) and the top contact electrode was deposited with nm precision over the position and shape by Focused Electron Beam Induced Deposition (FEBID) to give 'all-carbon' electrode molecular electronic devices.

Key Words: Molecular Electronics, Langmuir-Blodgett, FEBID

Abstract

Nascent molecular electronic devices, based on monolayer Langmuir-Blodgett (LB) films sandwiched between two carbonaceous electrodes, have been prepared. Tightly-packed monolayers of 4-((4-((4-ethynylphenyl)ethynyl)phenyl)ethynyl)benzoic acid were deposited onto a highly oriented pyrolytic graphite electrode. An amorphous carbon top contact electrode was formed on top of the monolayer from a naphthalene precursor using the Focused Electron Beam Induced Deposition technique. This allows the deposition of a carbon top-contact electrode with well-defined shape, thickness, and precise positioning on the film with nm resolution. These results represent a

substantial step towards the realization of integrated molecular electronic devices based on monolayers and carbon electrodes.

Introduction

Molecular electronics, in which a single molecule or a single layer of molecules is oriented between two immobile electrodes[1] to create a nascent, nanometer-sized device which harnesses the electrical properties of the molecular component[2] is an exciting area of science and an emerging technology base. The use of functional molecules capable of working as molecular wires,[3] rectifiers, [4] molecular switches,[5] etc. may provide many benefits to the electronic industry[6] including the overcoming of the difficulties associated with top-down scaling of conventional silicon technology and provide new avenues to increase device density,[2,6] as well as the introduction of new chemically-derived functionalities[7] and electronic properties due to the quantum effects that appear at the scale of atoms and molecules.[8]

The field of molecular electronics has been driven through the development of experimental methods for assessing the electrical properties of molecules in contact with two electrodes. This has in turn led to immense interest in molecular 'anchoring' groups to contact the molecule to the electrode surface, the nature of the electrode-molecule contact and the effects of contact resistance on the overall device performance. Much of the contemporary work in the area has concerned the electrical properties of single molecules contacted with metallic, often gold, electrodes. However, in the last few years, both the methods for contacting larger area films of molecular components into device-like structures more compatible with conventional fabrication strategies and the use of non-metallic electrodes have attracted growing attention.[9] Additionally, there is a growing interest in the construction of carbon based (opto)electronic devices[10] avoiding the use of rare and expensive metals as well as potentially toxic materials that result in electronic waste or e-waste.[11]

McCreery and co-workers[9a,9c,12] have elegantly addressed these topics and characterized the electronic properties of molecular bilayers[9c] or thin multilayers[9a,12b] sandwiched between two carbonaceous conducting electrodes. In this seminal work, a carbon-based top contact electrode was deposited by e-beam deposition from pure graphite using shadow masks to obtain regular-shaped carbon features (C-stamps) onto the organic film.[9a] However, extension of the method to the e-beam deposition of the top-contact carbon based electrode onto diazonium-grafted monolayer films arranged onto graphite-like surfaces resulted in short-circuited devices due to the frequent occurrence of defects and pinholes in the organic layers.[9c] Indeed, many deposition strategies for the assembly of the 'top-contact' onto monolayer films suffer from such interpenetrations through defects in the film, or result in damage to the underlying layer.[13]

The establishment of new methods for the shape and location specific deposition of 'top-contact' electrodes onto monolayers of electrically functional molecules that avoid film damage or penetration, would be an obvious milestone on the roadmap to the development of scalable molecular electronic devices. The use of simple, reliable and *in situ* methods for the measurement of the electrical properties of the resulting sandwich-like assemblies would also be beneficial during the development process of such prototypical electronic devices. In this paper, we report the fabrication of molecular electronic devices derived from molecular monolayers with all-carbon electrodes. Each single device has a top-electrode of controllable area and shape, and multiple devices can be constructed over a single substrate with control of the spatial arrangement. Thus, a carbon-based top contact is precisely deposited by Focused Electron Beam Induced Deposition (FEBID) onto a Langmuir-Blodgett (LB) monolayer of a densely assembled organic material onto a highly oriented pyrolytic graphite (HOPG) substrate. Figure 1 illustrates the fabrication process of these all-carbon electrode molecular electronic devices. A two-wire microprobe station was used to accurately locate

the probes that permit *in situ* electrical characterization of these nascent devices. In this way, deposition of a metal interconnects is not required for electrical assessment, revealing that the reliability of the fabrication process is high with a low occurrence of short-circuits.

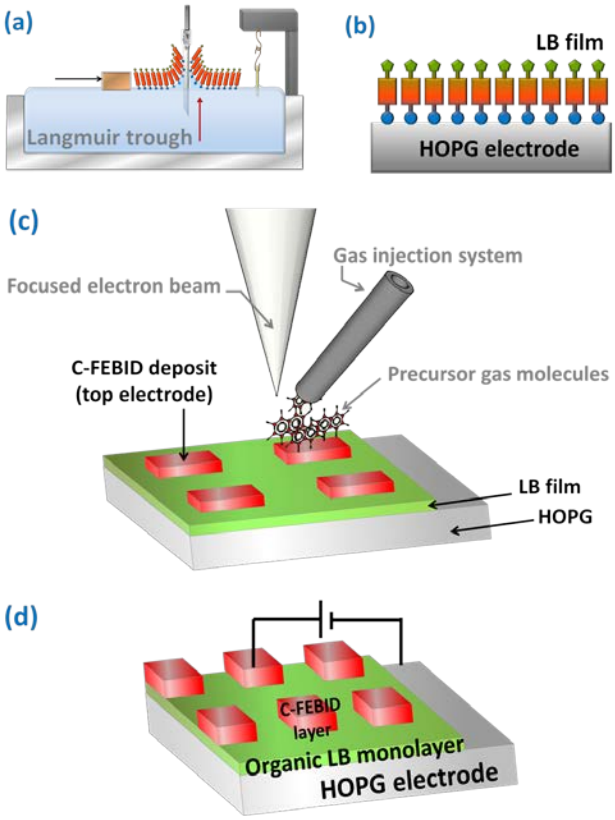

Figure 1. Sketch of the fabrication process of all-carbon electrode molecular electronic devices by carbon FEBID deposition onto a monolayer LB film. (a) Langmuir film at the air-water interface and scheme of the transference process onto HOPG by withdrawal of the electrode from the water subphase. (b) Monolayer LB film deposited onto an HOPG electrode. (c) FEBID is an additive lithography technique where the precursor (naphthalene, $C_{10}H_8$) is delivered onto the surface by a nearby gas injection system. As the focused beam is scanned, it dissociates locally the precursor gas molecules, creating a deposit with the same shape of the beam scan. (d) 3D view of all-carbon electrode molecular electronic devices.

Results and discussion

The initial stage of device fabrication commenced with deposition of a highly-ordered and tightly-packed monolayer LB film of 4-((4-((4-ethynylphenyl)ethynyl)phenyl)ethynyl)benzoic acid (**1**)[14] onto a HOPG electrode (Figure 2). A thorough characterization of a monolayer LB film of **1** has been previously reported.[14] In contrast with the self-assembly (SA) technique, no specific chemical interactions between the substrate and the molecules are required for LB film formation. Therefore, by making use of the wide variety of functional groups that can be physically adsorbed onto different substrates, it is possible to use LB methods to fabricate structures featuring any one of a large number of organic-electrode interfaces.[15] HOPG electrodes exhibit exceptionally flat surfaces and therefore the morphology of monolayers deposited onto HOPG can be studied in detail by Atomic Force Microscopy (AFM).

Figure 2 shows a representative AFM image of a monolayer film of **1** onto HOPG, illustrating the highly homogeneous and tightly-packed monolayer LB film of **1**, with a low density of holes, three dimensional aggregates and defects. In addition, the film closely follows the topography of the entirely covered underlying substrate and characteristic features of the HOPG substrate, such as steps and terraces, remain visible through the LB film. The monolayer LB film of **1** exhibits a low RMS (root mean square) roughness of 0.44 ± 0.07 nm (Figure S2 in the Supporting Information). The thickness of the LB film was determined by scratching the film with the AFM tip[16] which resulted in a 2.1 ± 0.3 nm film thickness (Figure S3 in the Supporting Information), which is in very good agreement with the molecule length of **1** (2.1 nm) determined from molecular models (Spartan 08 V1.0.0), and consistent with these molecules being assembled into a 2D arrangement normal to the surface.

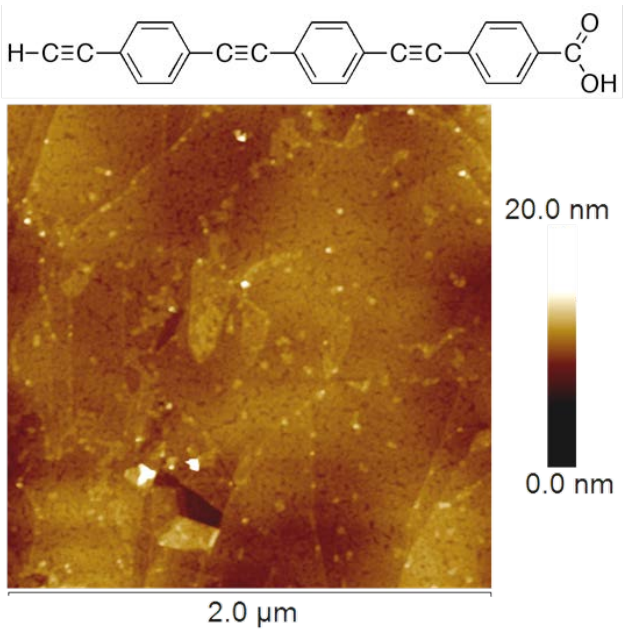

Figure 2. Top: molecular structure of 4-((4-((4-ethynylphenyl)ethynyl)phenyl)ethynyl)benzoic acid, **1**. Bottom: 2.0 x 2.0 µm^2 AFM image showing the topography of a monolayer LB film of **1** on a HOPG substrate.

Most large area devices in the field of nanoelectronics and molecular electronics are fabricated in a top-down approach, which entails the use of micro- and nano-lithography techniques to create the 'top-contact' to the molecular film.[13b,17] FEBID is an additive lithography technique where precursor molecules delivered by a gas-injection system become adsorbed onto a surface and are dissociated by back-scattered and secondary electrons produced by interaction of a focused electron beam with the substrate, creating a local deposit with the same shape of the scanning beam, thereby avoiding the use of resists, masks and etches (Figure 1c). By exercising control over the precursor and e-beam, it is possible to use this process to grow carbonaceous deposits with tailored shapes,[18] and structures such as carbon supertips[19] or carbon nanotweezers[20] have been prepared in this way. The use of such carbonaceous deposits for the creation of low resistance electrical connections to carbon-based nanostructures has been demonstrated,[21] as has the use of this technology to tailor the

contact resistance between graphene and metals.[22] A related approach is to introduce the precursor molecules in a controlled manner through a gas-injection system. This permits not only selection and use of well-defined precursor molecules, but also allows control of their flux within the chamber that in turn helps to control the deposition parameters and outcome. A variety of precursor molecules has been used to date for different applications, which have been reviewed elsewhere,[23] including carbon deposition from organic precursors.[24] In the work presented here, naphthalene ($C_{10}H_8$) has been employed as a precursor, resulting in deposition of an amorphous carbon layer (hereafter called a C-FEBID layer) the properties of which are reported in detail in the Supplementary Data. This amorphous carbon deposit shows suitable properties to establish electrical contacts to monolayer organic films.

The carbon top electrode of the devices was obtained by introducing the naphthalene precursor as a gas, which produces a controlled carbon-based nanodeposit (C-FEBID) after its dissociation by the focused electron beam under a voltage acceleration of 5 kV and using a 26 nA beam current. The electrical resistivity of these carbon C-FEBID nanodeposits was measured as (5.2 ± 0.1) × 10^5 μΩ·cm (see Supporting Information for further details: Figures S4 and S5). Examination of the structure, morphology and thickness of the C-FEBID-patterned top-contact electrode was also conducted by TEM and AFM (Figures S2, S6 and S7 in the Supporting Information). According to the AFM images and the height profiles registered for different carbon squares patterned in the same substrate and also in distinct but equivalent samples, the obtained area and thickness of the carbon layer deposited by FEBID were 5 × 5 μm^2 and 49 ± 4 nm, respectively. Taking into account these dimensions and the electrical resistivity value of these nanodeposits, the top-electrode resistance is about 10.2 Ω, much lower than the resistance of the LB film, which ensures uniform current flow across the device. In addition, AFM imaging conducted on top of the C-FEBID patterned squares

shows a very smooth, compact and homogeneous carbon layer (Figure S7 in the Supporting Information), substantially free of pinholes, defects and large 3D aggregates. Indeed, after carbon deposition, the RMS of the area masked by the top contact decreased to 0.30 ± 0.02 nm (Figure S2 in the Supporting Information).

The electrical properties of the resulting sandwich-like all-carbon electrode molecular electronic devices were determined by contacting two *in situ* electrical microprobes. Figure 3 shows the (artificially colored) SEM micrograph of a monolayer LB film of **1** on HOPG with red regions indicating the three all-carbon electrode molecular electronic devices fabricated on top of the LB film and blue regions indicating the *in situ* electrical microprobes. One of the electrical microprobes was placed on the top electrode and the second one provided electrical contact to the bottom electrode, i.e. to a clean area of the HOPG substrate.

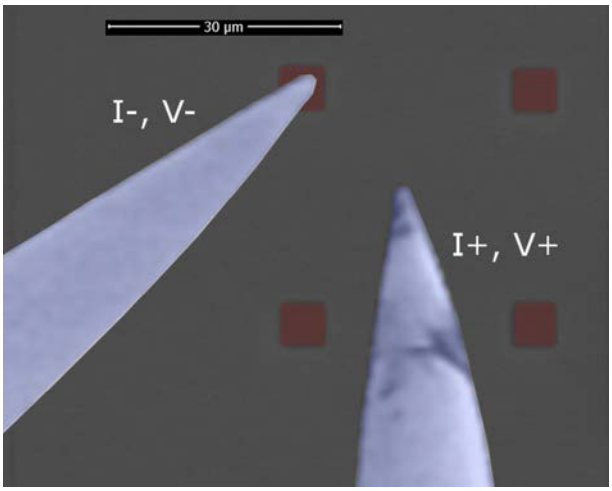

Figure 3. Artificially colored SEM micrograph of a monolayer LB film of **1** grown on HOPG, containing four all-carbon electrode devices, with red regions indicating the four carbon top electrodes and blue regions indicating the *in situ* electrical microprobes.

Figure 4 shows current density vs. voltage curves, *J-V* curves, obtained for three different devices, fabricated on three different monolayer LB films of **1** each transferred onto different HOPG substrates. The measurements on these three distinct devices are similar (Figure 4), demonstrating the high reproducibility of the different steps involved in the fabrication process. Additionally, control experiments were done by recording the *J-V* curves of a C-FEBID deposit onto a HOPG substrate (without the monolayer in between both electrodes: red curve in Figure 5) to verify that the observed electrical properties are due to the HOPG/monolayer/C-FEBID devices. This control experiment also permits to rule out both the degradation of the organic monolayer of **1** into amorphous carbon by the electrons of the FEBID process and short-circuiting due to possible/ hypothetical pinholes and defects occurring in the LB film of **1**. The experimental *J-V* curves for the HOPG/monolayer/C-FEBID exhibit a linear response in the -0.7 V - +0.7 V voltage range and a nonlinear behavior for higher bias voltages. The nonlinear transport across **1** has been previously observed,[14] with Scanning Tunneling Microscopy (STM) experiments showing that the transport through individual **1** molecules can be modeled in terms of transport across a tunneling barrier, by the Simmons expression:[25]

$$J = \frac{e}{4\pi^2\hbar s^2}\left\{\left(\Phi - \frac{eV}{2}\right)\exp\left[-\frac{2(2m)^{1/2}}{\hbar}\alpha\left(\Phi - \frac{eV}{2}\right)^{1/2}s\right] - \left(\Phi + \frac{eV}{2}\right)\exp\left[-\frac{2(2m)^{1/2}}{\hbar}\alpha\left(\Phi + \frac{eV}{2}\right)^{1/2}s\right]\right\} \quad (1)$$

s is the width of the tunneling barrier, Φ is the effective barrier height of the tunneling junction, *V* is the potential applied to the junction, α is a parameter related to the effective mass of the electrons in the tunneling process and *e* and *m* are the charge and the mass of the electron. Solid lines in Figure 4 are the best fits obtained by using Equation 1 with the width of the tunneling barrier *s* being the value determined in the AFM experiments, 2.1 nm, and allowing Φ and α to behave as free parameters. For the three *J-V* curves shown in Figure 4, the best agreement between the experimental *J-V* curves and

the Simmons model is found for Φ = 2.05 eV (a), 2.00 eV (b), 2.01 eV (c) and α = 0.41 (a - c). The values obtained for the effective tunneling barrier height modeling the transport across the devices based on LB films of **1** are relatively high, and of the same order of magnitude of the work function values in HOPG and C, around 5 eV. This implies that all the interfaces present in the devices are clean and flat and the LB film forming the tunneling barrier is compact and almost defect-free: only when having a defect-free tunneling barrier as well as clean and flat interfaces in the junction, the effective tunneling-barrier height determined experimentally approaches that of the work function (a reduction of 50% in magnitude can reasonably be attributed to image potential and corrugation effects).[26]

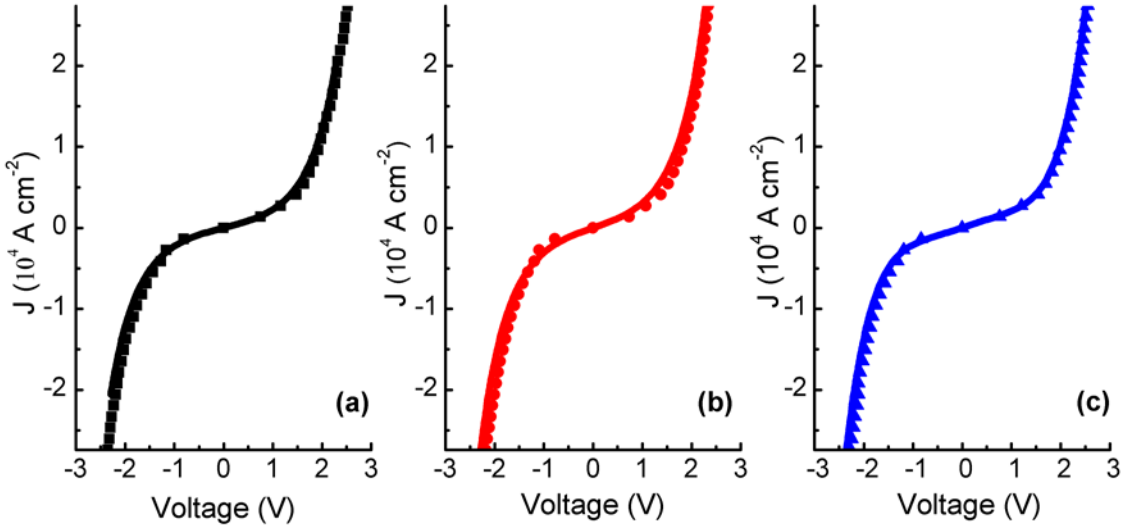

Figure 4. *J-V* curves of three all-carbon electrode molecular electronic devices (a, b, c) fabricated on three different monolayer LB films of **1** transferred onto HOPG, stressing the reproducibility in the growth of both the LB films and the top contact by FEBID. The standard deviation of the experimental voltage values is 0.01 V. Solid lines are fittings to the Simmons equation with Φ = 2.05 eV (a), 2.00 eV (b) and 2.01 eV (c), and α = 0.41.

In order to guarantee the reproducibility and the robustness of the fabrication process, twenty-four devices were fabricated on different regions of six separately formed LB films of **1**, only three of which were short-circuited. The *J-V* curves of each of the other twenty-one functional devices

were determined from different positions on the top electrode by carefully placing *in situ* the electrical microprobe with the aid of the SEM. The *J-V* curves measured on the devices fabricated onto different regions of the same monolayer LB film of **1** are similar. The measurements of each functional device are also fully reproducible on two different positions of the top contact electrode, and the resulting forty-two measurements from across the range of devices can be fitted to the Simmons model (Equation 1, inset of Figure 5) with fixed width of the tunneling barrier (2.1 nm) and Φ and α as free parameters. These curves are collected in Figure 5. The values found for the effective tunneling barrier height, Φ, in the fitting of each *J-V* curve measured are plotted in the inset of Figure 5. The spread in the values of the effective tunneling barrier height for each sample, (2.02 ± 0.02) eV, is extremely low, indicating the reproducibility and the robustness of the fabrication process of the all carbon electrode devices. The statistical distribution of the rectification ratio values has also been obtained. The rectification value is defined as the ratio between the current densities at the maximum positive and negative voltages. The histogram of the rectification ratio values constructed from the data of all the devices fabricated in this work (Figure S9 of the Supporting Information) shows a very small spreading in the values, which suggest a very good reproducibility among all the devices.

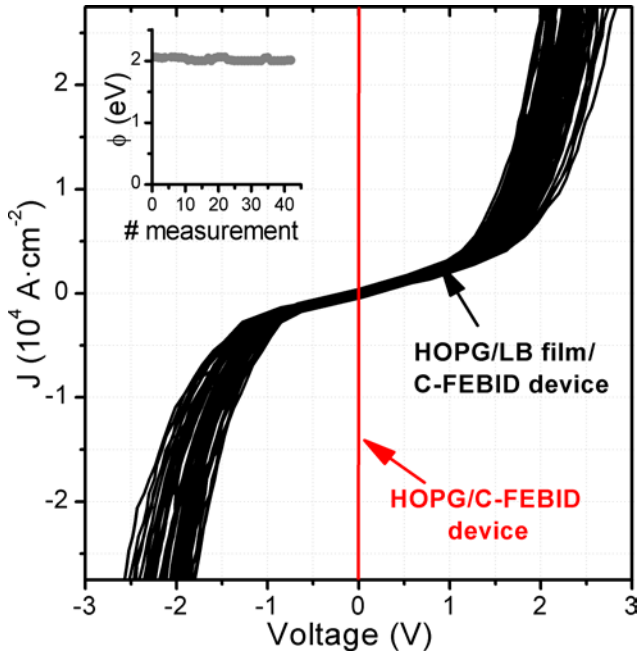

Figure 5. *J-V* curves measurements of twenty-one different all-carbon electrode molecular electronic devices (HOPG/monolayer LB film of **1**/C-FEBID top contact electrode. The figure includes two *J-V* curves per device, i.e., a total of 42 *J-V* curves. The standard deviation of the experimental voltage values is 0.01 V. The red line corresponds to the curve obtained for a HOPG/C-FEBID device, without the monolayer LB film of **1** between the two electrodes. The inset figure shows the values obtained for the effective barrier height of the tunnelling transport across the all-carbon electrode molecular electronic devices in all the measurements performed.

Conclusion

In this contribution, FEBID has been used to fabricate small area top-contact carbon electrodes on tightly packed monolayer LB films supported on HOPG substrates allowing the production of robust all-carbon electrode based electronic devices. The devices fashioned in this way exhibit high reproducibility in their electrical properties. These carbon-based nanoelectronic devices

arise from a metal-free top contact carbon based electrode, which can be deposited without the need of resists nor masks, with the location, shape and size of the C-FEBID deposit determined by the path of the e-beam. The low-cost carbon precursor avoids the use of expensive and scarce metals or metal oxides, while the deposition process avoids atomic diffusion and quenching phenomena common to metal-top-contact based opto-electronic devices. The proof-of-concept demonstrated here paves the way for further advances in the development of electronic devices based on the combination of LB films and carbon-based electrodes. Since the FEBID technique is capable of very high lateral resolution (a few nm), further advances towards ultra-miniaturized devices should prove possible;[27] work towards these goals is now underway.

Experimental

The synthesis of 4-((4-((4-ethynylphenyl)ethynyl)phenyl)ethynyl)benzoic acid, **1,** has been reported elsewhere.[14] Langmuir films of **1** were prepared on a Nima Teflon trough with dimensions (720x100) mm^2, which was housed in a constant temperature (20 ± 1 ºC) clean room. A Wilhelmy paper plate pressure sensor was used to measure the surface pressure (π) of the monolayers. The sub-phase was an aqueous (Millipore Milli-Q, resistivity 18.2 MΩ·cm) solution of NaOH whose pH was 9, which reduces the formation of 3D aggregates at the air-water interface. A solution of **1** in hexane:ethanol (2:1) (both solvents purchased from Aldrich and used as received; purity HPLC grade 99% and >99.5%, respectively) was delivered from a syringe held very close to the surface, allowing the surface pressure to return to a value as close as possible to zero between each addition. Hexane was employed as the spreading solvent since **1** is not soluble in other common solvents used in the Langmuir-Blodgett technique (e.g. chloroform). The use of ethanol in the spreading solvent serves to limit the formation of hydrogen-bonded carboxylic acid dimers and aggregates in solution prior to deposition. The spreading solvent was allowed to completely evaporate from the surface of the sub-

phase over a period of at least 20 min before compression of the monolayer commenced at a constant sweeping speed of 0.015 $nm^2 \cdot molecule^{-1} \cdot min^{-1}$. The Langmuir monolayers of **1** were deposited onto HOPG electrodes at a constant surface pressure of 18 $mN \cdot m^{-1}$ by withdrawing the HOPG electrodes from the water subphase using the vertical dipping method and a dipping speed of 3 $mm \cdot min^{-1}$. In this way, compound **1** is connected to the HOPG electrode through the carboxylate group (Supporting Information).

Atomic Force Microscopy (AFM) experiments were performed by means of a Multimode 8 AFM system equipped with a Nanoscope V control unit from Veeco, operating in Tapping and Peak-Force modes. The data were collected with silicon cantilevers provided by Bruker, namely ScanAsyst-Air-HR (130–160 kHz, and 0.4–0.6 $N \cdot m^{-1}$) and RFESPA-75 (75-100 kHz, and 1.5–6 $N \cdot m^{-1}$). The images were collected with a scan rate of 0.5-1.2 Hz, an amplitude set point lower than 1 V, and in ambient air conditions. The electrical properties of the sandwich-like all-carbon electrode molecular electronic devices were determined by contacting two *in situ* electrical microprobes from Kleindiek, connected via a feed-through to a combined Keithley system featuring a 6220 dc current source and a 2182 nanovoltmeter located out of the microscope chamber.

Supporting Information

Supporting Information related to this article can be found at http:// (to be completed by the editorial office…)

Author Information

Corresponding Author

*Jose María de Teresa: deteresa@unizar.es

*Pilar Cea: pilarcea@unizar.es

Author Contributions

The manuscript was written through contributions of all authors. All authors have given approval to the final version of the manuscript. S.S., S.M, and A.G-O, contributed equally.

Acknowledgments

This work was supported by the Ministerio de Ciencia e Innovación from Spain in the framework of grants CTQ2013-50187-EXP, MAT2014-51982-C2-1-R, MAT2014-51982-C2-2-R, MAT2015-69725-REDT from MINECO (including FEDER funding) and CELINA COST Action CM1301. Financial support from DGA/Fondos Feder is also acknowledged by research group Platon (E-54) and Magna (E-26). P.J.L. holds an ARC Future Fellowship (FT120100073) and gratefully acknowledges funding for this work from the ARC (DP140100855). Authors also acknowledge Laura Casado, technician at the LMA, for her help in the FEBID experiments. We thank Dr Santiago Marqués-González for preparation of a sample of **1**.

References

[1] J. R. Heath, *Annu. Rev. Mater. Res.* **2009**, *39*, 1.
[2] Editorial, *Nat. Nanotech.* **2013**, *8*, 377.
[3] E. Leary, A. La Rosa, M. T. Gonzalez, G. Rubio-Bollinger, N. Agrait, N. Martín, *Chem. Soc. Rev.* **2015**, *44*, 920.
[4] a) A. Aviram, M. Ratner, *Chem. Phys. Lett.* **1974**, *29*, 277; b) G. Jayamurugan, V. Gowri, D. Hernández, S. Martín, A. González-Orive, C. Dengiz, O. Dumele, F. Pérez-Murano, J.-P. Gisselbrecht, C. Boudon, W. B. Schweizer, B. Breiten, A. D. Finke, G. Jeschke, B. Bernet, L. Ruhlmmann, P. Cea, F. Diederich, *Chem. Eur. J.* **2016**, *22*, 10539.
[5] C. Simao, M. Mas-Torrent, N. Crivillers, C. Lloveras, J. M. Artes, P. Gorostiza, J. Veciana, C. Rovira, *Nature Chem.* **2011**, *3*, 359.
[6] D. Xiang, X. Wang, C. Jia, T. Lee, X. Guo, *Chem. Rev.* **2016**, 4318.
[7] a) L. Bogani, W. Wernsdorfer, *Nat. Mater.* **2008**, *7*, 179; b) S. Sanvito, *Chem. Soc. Rev.* **2011**, *40*, 3336; c) Y. Kim, W. Jeong, K. Kyeongtae, W. Lee, P. Reddy, *Nat. Nanotech.* **2014**, *9*, 881.

[8] a) P. Reddy, S. Y. Jang, R. A. Segalman, A. Majumdar, *Science* **2007**, *315*, 1568; b) S. Iacovita, M. C. Rastei, B. W. Heinrich, T. Brumme, J. Kortus, L. Limot, J. P. Bucher, *Phys. Rev. Lett.* **2008**, *101*, 116602; c) R. Vincent, S. Klyatskaya, M. Ruben, W. Wernsdorfer, F. Balestro, *Nature* **2012**, *488*, 357; d) M. F. Gonzalez-Zalba, A. Saraiva, M. J. Calderón, D. Heiss, B. Koiller, A. J. Ferguson, *Nano Lett.* **2014**, *14*, 5672.

[9] a) H. Yan, A. J. Bergren, R. L. McCreery, *J. Am. Chem. Soc.* **2011**, *133*, 19168; b) J. P. Moscatello, A. Prasad, R. Chintala, K. K. Yap, *Carbon* **2012**, *50*, 3530; c) S. Y. Sayed, A. Bayat, M. Kondratenko, Y. Leroux, P. Hapiot, R. L. McCreery, *J. Am. Chem. Soc.* **2013**, *135*, 12972; d) S. Seo, M. Min, S. M. Lee, H. Lee, *Nat. Commun.* **2013**, *4*, 1920; e) P. Song, C. S. S. Sangeeth, D. Thompson, W. Du, K. P. Loh, C. A. Nijhuis, *Adv. Mater. Interf.* **2016**, *28*, 631.

[10] C. Jia, B. Ma, N. Xin, X. Guo, *Acc. Chem. Res.* **2015**, *58*, 2565.

[11] a) M. J. Tan, C. Owh, P. L. Chee, A. K. K. Kyaw, D. Kai, X. J. Loh, *J. Mater. Chem. C.* **2016**, 5531; b) M. Irimia-Vladu, *Chem. Soc. Rev.* **2014**, *43*, 588; c) P. Cea, L. M. Ballesteros, S. Martin, *Nanofabrication* **2014**, *1*, 96.

[12] a) J. Ru, B. Szeto, A. Bonifas, R. L. McCreery, *ACS. Appl. Mater. Interf.* **2010**, *2*, 3693; b) H. Yan, A. J. Bergren, R. L. McCreery, M. L. Della Rocca, P. Martin, P. Lafarge, J. C. Lacroix, *Proc. Natl. Acad. Sci. U.S.A.* **2013**, *110*, 5326.

[13] a) A. V. Walker, T. B. Tighe, J. Stapleton, B. C. Haynie, S. Upilli, D. L. Allara, N. Winograd, *Appl. Phys. Lett.* **2004**, *84*, 4008; b) D. Vuillaume, *Proc. IEEE* **2010**, *98*, 2111.

[14] a) L. M. Ballesteros, S. Martín, C. Momblona, S. Marqués-González, M. C. López, R. J. Nichols, P. J. Low, P. Cea, *J. Phys. Chem. C.* **2012**, *116*, 9142. b) H. M. Osorio, P. Cea, L. M. Ballesteros, I. Gascón, S. Marqués-González, R. J. Nichols, F. Pérez-Murano, P. J. Low, S. Martín, *J. Mater. Chem. C* **2014**, 2, 7348.

[15] a) G. Pera, A. Villares, M. C. Lopez, P. Cea, D. P. Lydon, P. J. Low, *Chem. Mater.* **2007**, *19*, 857; b) A. Villares, D. P. Lydon, L. Porres, A. Beeby, P. J. Low, P. Cea, F. M. Royo, *J. Phys. Chem. B.* **2007**, *111*, 7201; c) L. M. Ballesteros, S. Martín, G. Pera, P. A. Schauer, N. J. Kay, M. C. López, P. J. Low, R. J. Nichols, P. Cea, *Langmuir* **2011**, *27*, 3600.

[16] S. Ranganathan, R. L. McCreery, *Anal. Chem.* **2001**, *73*, 893.

[17] a) Y. N. Xia, J. A. Rogers, K. E. Paul, G. M. Whitesides, *Chem. Rev.* **1999**, *99*, 1823; b) J. I. Martin, J. Nogues, K. Liu, J. L. Vicent, I. K. Schuller, *J. Magn. Magn. Mater.* **2003**, *256*, 449.

[18] N. Miura, H. Ishii, J. Shirakashi, A. Yamada, M. Konagai, *Appl. Surf. Sci.* **1997**, *113*, 269.

[19] M. Castagne, M. Benfedda, S. Lahimer, P. Falgayrettes, J. P. Fillard, *Ultramicroscopy* **1999**, *76*, 187.

[20] P. Boggild, T. M. Hansen, C. Tanasa, F. Grey, *Nanotechnology* **2001**, *12*, 331.

[21] a) F. Banhart, *Nano Lett.* **2001**, *1*, 329; b) K. Rykaczewski, M. R. Henry, S. K. Kim, A. G. Fedorov, D. Kulkarni, S. Singamaneni, V. V. Tsukruk, *Nanotechnology* **2010**, *21*, 035202.

[22] a) I. Neumann, M. V. Costache, G. Bridoux, J. F. Sierra, S. O. Valenzuela, *Appl. Phys. Lett.* **2013**, *103*, 112401; b) S. Kim, D. D. Kulkarni, R. Davis, S. S. Kim, R. R. Naik, A. A. Voevodin, M. Russell, S. S. Jang, V. V. Tsukruk, A. G. Fedorov, *ACS Nano* **2014**, *8*, 6805; c) S. Kim, M. Russell, M. Henry, S. S. Kim, R. R. Naik, A. A. Voevodin, S. S. Jang, V. V. Tsukruk, A. G. Fedorov, *Nanoscale* **2015**, *7*, 14946; d) S. Kim, M. Russell, D. D. Kulkarni, M. Henry, S. Kim, R. R. Naik, A. A. Voevodin, S. S. Jang, V. V. Tsukruk, A. G. Fedorov, *ACS Nano* **2016**, *10*, 1042.

[23] a) S. J. Randolph, J. D. Fowlkes, P. D. Rack, *Crit. Rev. Solid State* **2006**, *31*, 55; b) W. F. van Dorp, C. W. Hagen, *J. Appl. Phys.* **2008**, *104*, 081301; c) I. Utke, P. Hoffmann, J. Melngailis,

J. Vac. Sci. Technol B **2008**, *26*, 1197; d) M. Huth, F. Porrati, C. Schwalb, M. Winhold, R. Sachser, M. Dukic, J. Adams, G. Fantner, *Beilstein J. Nanotechnol.* **2012**, *3*, 597; e) J. J. L. Mulders, *Nanofabrication* **2014**, *1*, 74; f) J. M. De Teresa, A. Fernandez-Pacheco, R. Cordoba, L. Serrano-Ramon, S. Sangiao, M. R. Ibarra, *J. Phys. D Appl. Phys.* **2016**, 243003.

[24] T. Bret, S. Mauron, I. Utke, P. Hoffmann, *Microelectron Eng.* **2005**, *78-79*, 300.

[25] J. G. Simmons, *J. Appl. Phys.* **1963**, *281*, 1793.

[26] N. Garcia, *IBM J. Res. Dev.* **1986**, *30*, 533.

[27] W. F. van Dorp, B. va Someren, C. W. Hagen, P. A. Kruit Pand Croxier, *Nano Lett.* **2005**, 1303.